Deformation Behaviour of Clays under Sustained Load

by

N. S. Pandian*

B.V. Ranganatham**

Introduction

Soil by the very nature of its character is susceptible to and influenced by time element. Creep phenomena can occur in all the three fundamental stress-strain relations (i.e. hydrostatic, one dimensional and triaxial consolidations). From the nature of the stress-strain relations, it may be expected that creep under hydrostatic stress conditions would be of relatively less importance than that under triaxial stress change. Furthermore, hydrostatic and one dimensional consolidations would react as "self limiting systems" with regard to consolidation creep owing to the progressive reduction in volume with stress. Deformation creep in the triaxial case (i.e. with deviatoric loading) can persist at a constant rate indefinitely, unless someconsolidation does actually take place simultaneously to limit creep to some degree.

Earlier Work Done

The complex nature of the creep problem has made it difficult to evolve completely mathematical analysis and the time element made it cumbersome to make detailed experimental studies. Consequently the formulation of mathematical models based on limited experimental results has become inevitable. Many research workers have proposed models to explain the creep behaviour of soils. Awtar Singh and Mitchell (1968) suggested a three parameter phenomenological equation to describe strain-rate-time and strain-time response of clays under sustained loading based on their experimental observations. Kavazanjian and Mitchell (1980) have developed a constitutive model for the creep behaviour of cohesive soils by unifying the existing phenomenological models. Sekiguchi (1984) has proposed a elastoplastic model for the undrained creep rupture of normally consolidated clays.

*Assistant Professor, ⎫ Department of Civil Engineering, Indian Institute of
**Professor, ⎭ Science, Bangalore 560 012, India

It should be noted that to be of practical use in providing a generalized description of the creep characteristics of soils, any proposed relationship should satisfy the following (i) it must be applicable to a reasonable range of creep stresses; (ii) it must describe the behaviour of a range of soil types; (iii) it must account for both linear and nonlinear relationships between strain and time; and (iv) it must also contain parameters that are easily determined.

Guided by these considerations an experimental programme has been planned and carried out. In the analysis of the test data, a simple pheno-menological relationship has been observed which appears to describe quite satisfactorily the creep behaviour of soils. Using the above described relationship, the undrained creep behaviour of clays relating creep rate with time in terms of stress ratio (σ_1/σ_3) has been studied.

Experimental Programme

Kaolinite and montmorillonite soils were chosen for the study so as to cover a wide range of clay behaviour. They were mixed with 45% and 240% water contents respectively so as to give the required consistency for use in triaxial tests and kept in an air tight container for 5 days to ensure moisture distribution. Remoulded and saturated samples of 3.81 cm diameter and 7.62 cm height were obtained and consolidated in triaxial cells to the required pressure levels, viz., 0.7, 1.4, 2.1 and 2.8 kg/cm². Complete saturation was ensured by checking the pore pressure coefficient B to be equal to one. Then additional loads were added through a hanger so as to have the required total stress ratio when no drainage was permit-ted. Under this sustained loading, vertical deformation gauge readings were recorded at stated time intervals for about a month. Three samples were tested for each condition and the best average of the results abstracted for analysis. The soils used are commercially pure kaolinite and mont-morillonite, the index properties of which are;

	LL (%)	PL (%)	PI (%)
Kaolinite	68	39	29
Montmorillonite	630	85	545

The samples were covered by two rubber membranes to avoid possible leakage of water, the confining fluid. The room temperature was around 27°C.

Basic Considerations

The time deformation behaviour of saturated clayey samples under sustained deviatoric loading could be broadly described as shown in Fig.

1. Immediately upon the application of load, a rapid initial deformation takes place. This is followed by a progressively decreasing deformation rate designated as the primary or strain hardening stage which in turn is followed by a flow either of a constant speed or of decreasing speed depending upon the level of deviatoric loading. The rate of decrease of deformation is much slower compared to that at the primary stage. This is known as secondary or steady state creep. In the final stage (tertiary creep), the creep rate progressively increases with time leading to failure (curve 3) provided the level of deviatoric loading is equal to or greater than the creep strength of the sample. At lower deviatoric loading level, the tertiary stage may not be reached (curves 1 and 2) or creep may cease completely after some time (curve 1).

Strain-time Function

The plot of natural strain (natural strain $\bar{\epsilon} = -\log_e (1-\epsilon)$ where ϵ = ordinary strain = $\Delta 1/1_o$ in which Δ_1 is the change in length of a specimen of original length 1_o) versus time in a log-log scale (Typical Figs. 2 to 3) is found to be linear irrespective of whether the clay tested is kaolinite or montmorillonite. In what follows in this paper, unless otherwise stated, strain $\bar{\epsilon}$ refers to natural strain. These relationships (Figs. 2 to 3) can be expressed by

$$\log_e \bar{\epsilon} = m \log_e t + \log_e C \tag{1}$$

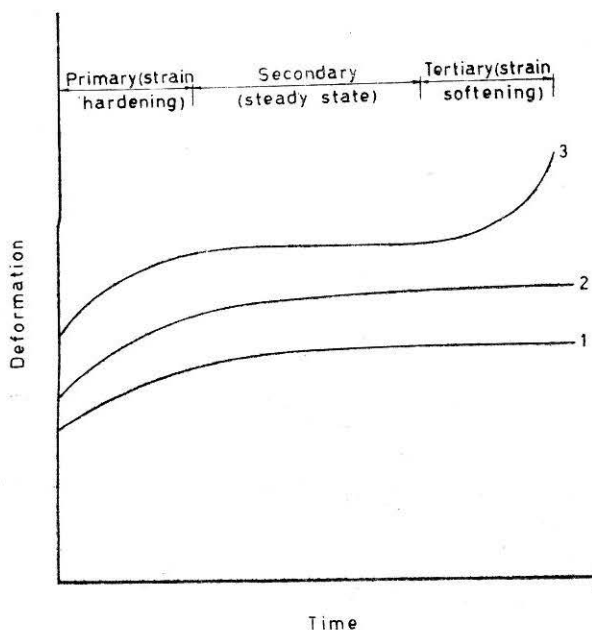$$\text{or} \quad \bar{\epsilon} = C t^m \tag{2}$$

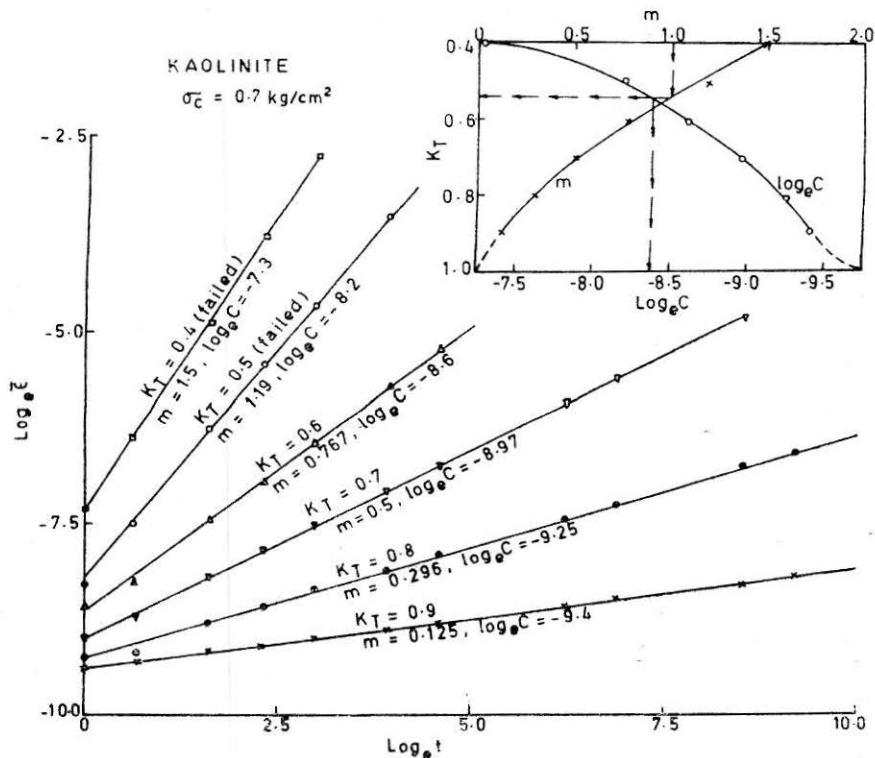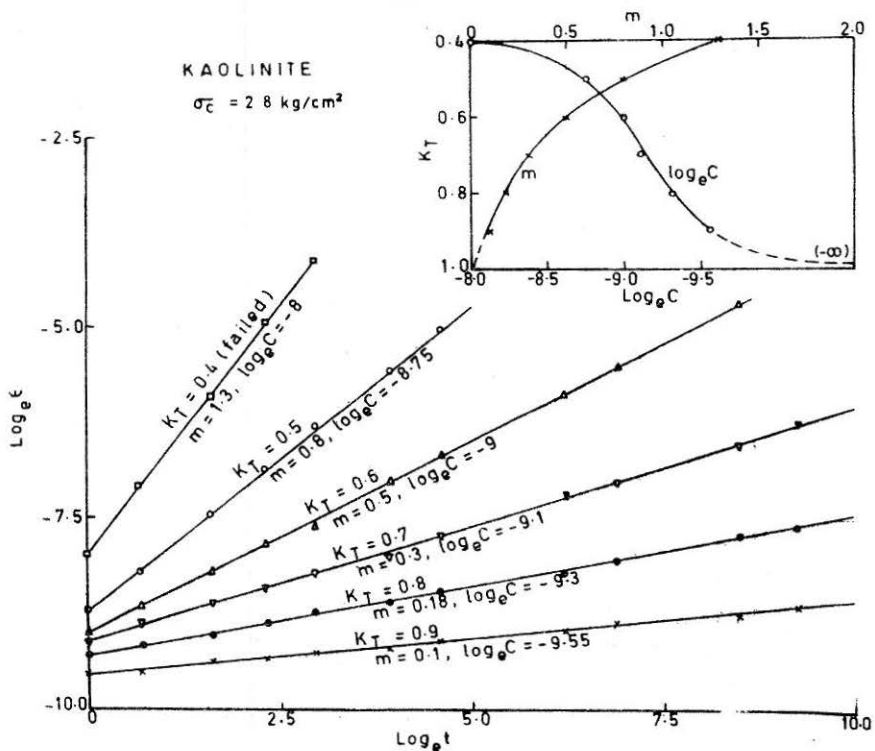FIGURE 1 Schematic Representation of Creep

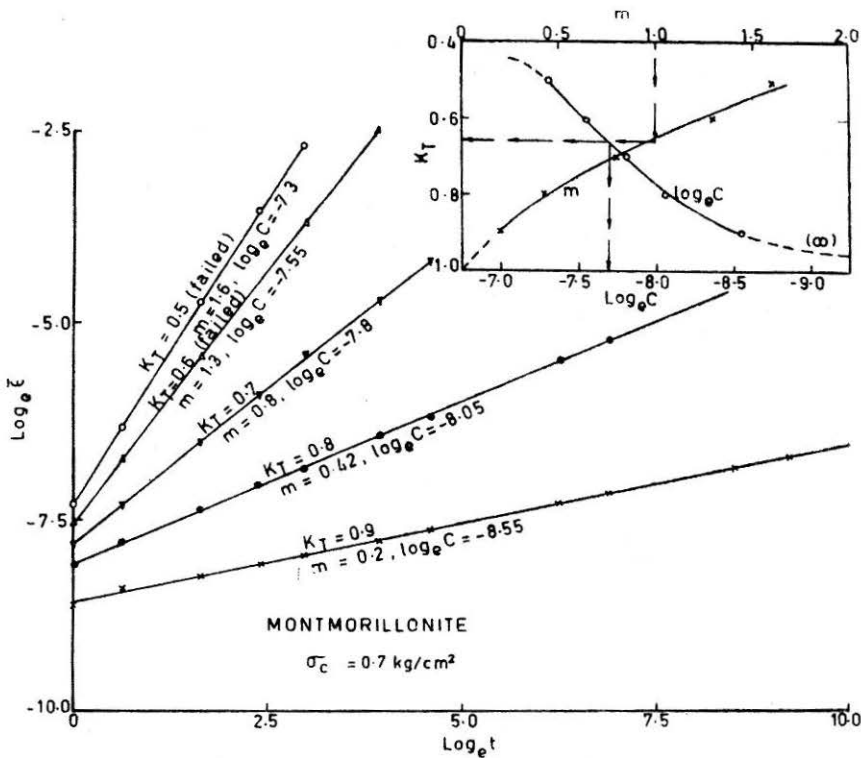FIGURE 2(a) Strain-Time Plot

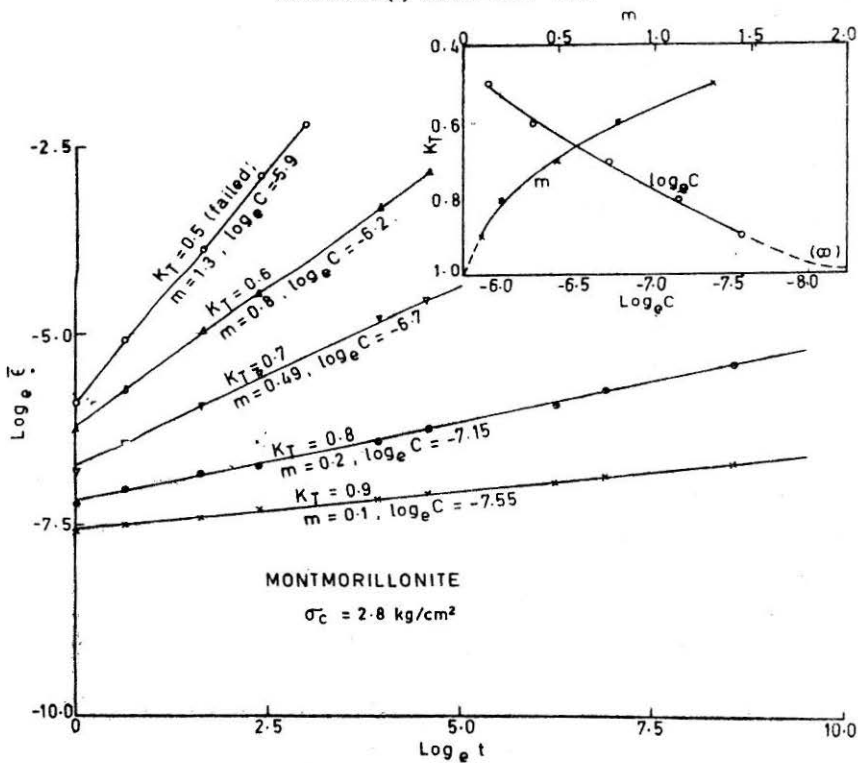FIGURE 2(b) Strain-Time Plot

FIGURE 3(a) Strain-Time Plot

FIGURE 3(b) Strain-Time Plot

in which t=time, in minutes, elapsed after the addition of the deviatoric loading which is kept constant; m=slope of the striaght line whose magnitude is found to increase with increasing intensity of deviatoric loading; and C is a constant.

Interpretation of Strain-Time Function

The physical implications of the empirically deduced functional relation $\bar{\epsilon} = Ct^m$ is herein attempted. Differentiating with respect to time, it yields

$$\frac{d\bar{\epsilon}}{dt} = \dot{\bar{\epsilon}} = C m \, t^{m-1}$$

$$= \text{strain rate} \tag{3}$$

Case (i) $m<1$: When m is less than unity, $(m-1)$ is negative and so with increasing values of t, the magnitude of the expression on the right hand side goes on decreasing. In other words, the strain rate goes on decreasing.

Case (ii) $m=1$: In this case $(m-1)$ is zero and so the magnitude of the expression on the right hand side is unaffected by t. In other words, it is the case of constant strain rate of magnitude C. The ratio of normal total stress (σ_1) to the ambient cell pressure (σ_3) (*i.e.* (σ_1/σ_3), referred to as K_T corresponding to the "$m=1$ case" is known as "critical creep stress ratio, $(K_T)_{cr}$". It may be explicity stated that since the ratio K in literature generally refers to the ratio of minor to major principal effective stresses and since what is referred to in this paper is the ratio in terms of total stresses, K_T is used to distinguish it. The critical values of K_T are found by plotting K_T against m, vide insets in Figs. 2 to 3. (In the test as well as figures, both σ_3 and σ_c have been used to denote cell pressures).

Case (iii) $m>1$: In this case, $(m-1)$ is positive and so with increasing values of t, the magnitude of the expression on the right hand side goes on increasing. In other words, the strain rate goes on increasing.

Relationship Between $\dot{\bar{\epsilon}}$ and K_T

Using the straight line plots between logarithm of natural strain and logarithm of time, the values of parameters C and m are determined and with the use of these two, the strain rate at a particular time for a specified K_T could be obtained. The plot of stress ratio K_T on the natural scale (as abscissa) and the strain rate $\dot{\bar{\epsilon}}$ on the logarithmic scale (as ordinate) yields a linear relation (typical plots shown in Figs. 4 and 5. All these straight lines are found to meet at a point $(K_T)_{cr}$, $\dot{\bar{\epsilon}}_{cr})$ where the value of K_T equals the critical one, $(K_T)_{cr}$ and the rate of strain corresponds to that which is obtained when $m=1$, i.e., $\dot{\bar{\epsilon}}_{cr}$.
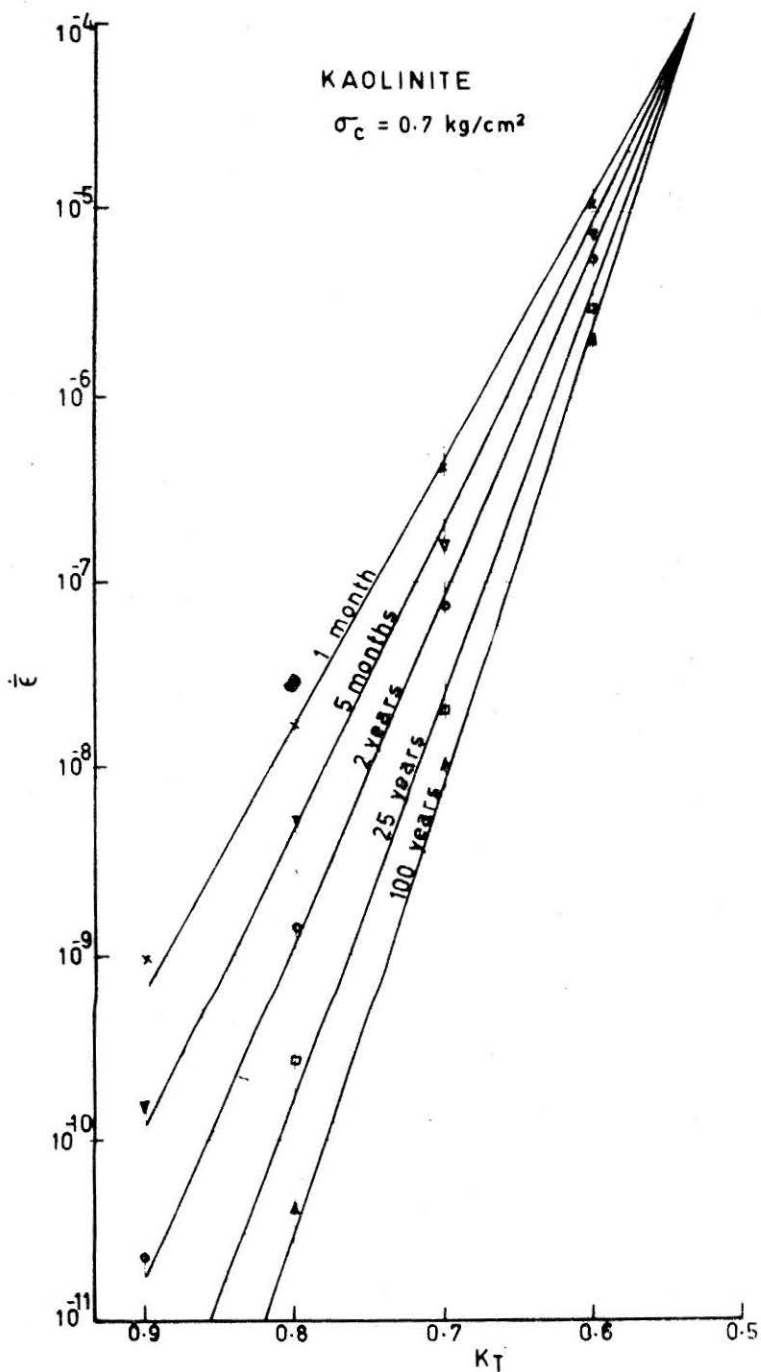
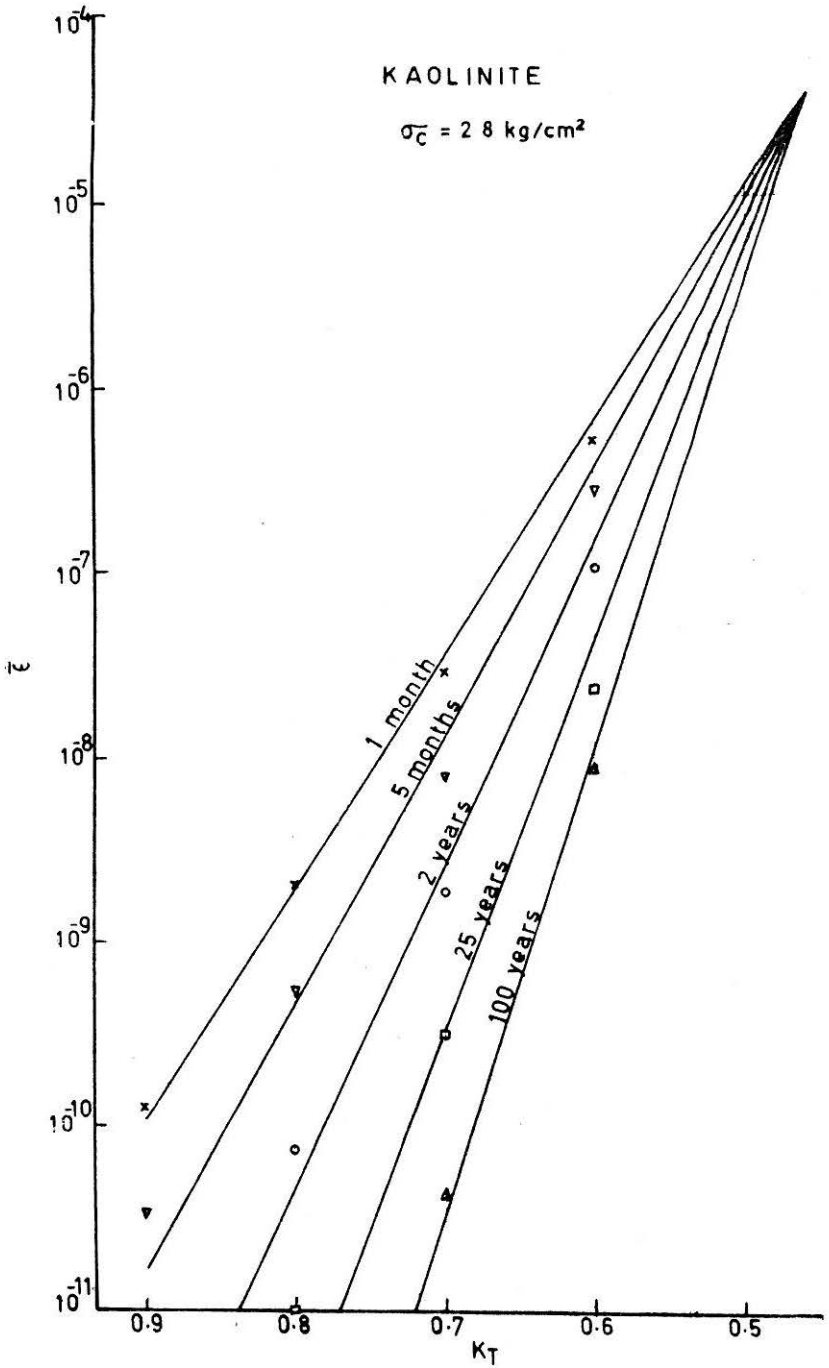FIGURE 4(a) Strain Rate—Stress Ratio Plot

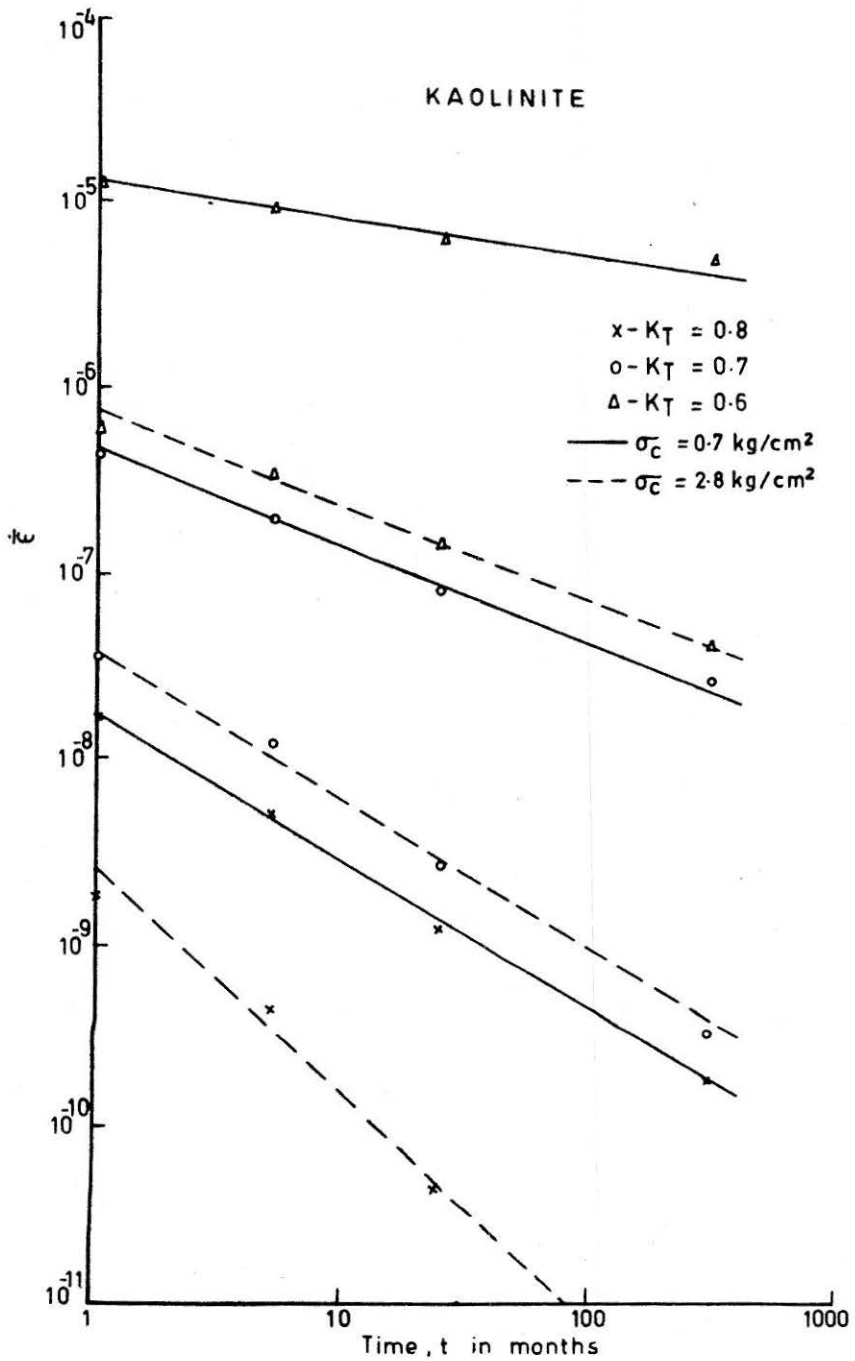FIGURE 4(b) Strain Rate—Stress Ratio Plot

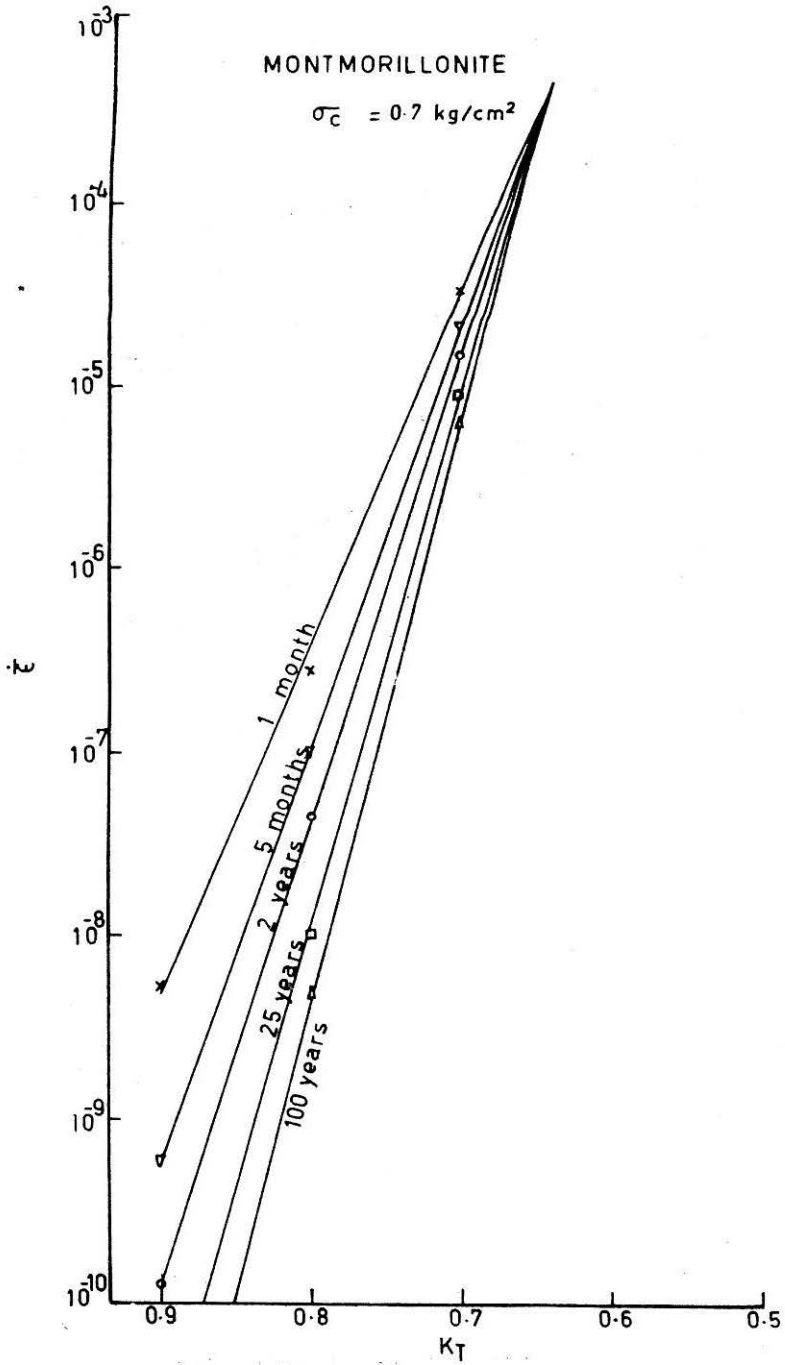FIGURE 4(c) Strain Rate—Time Plot
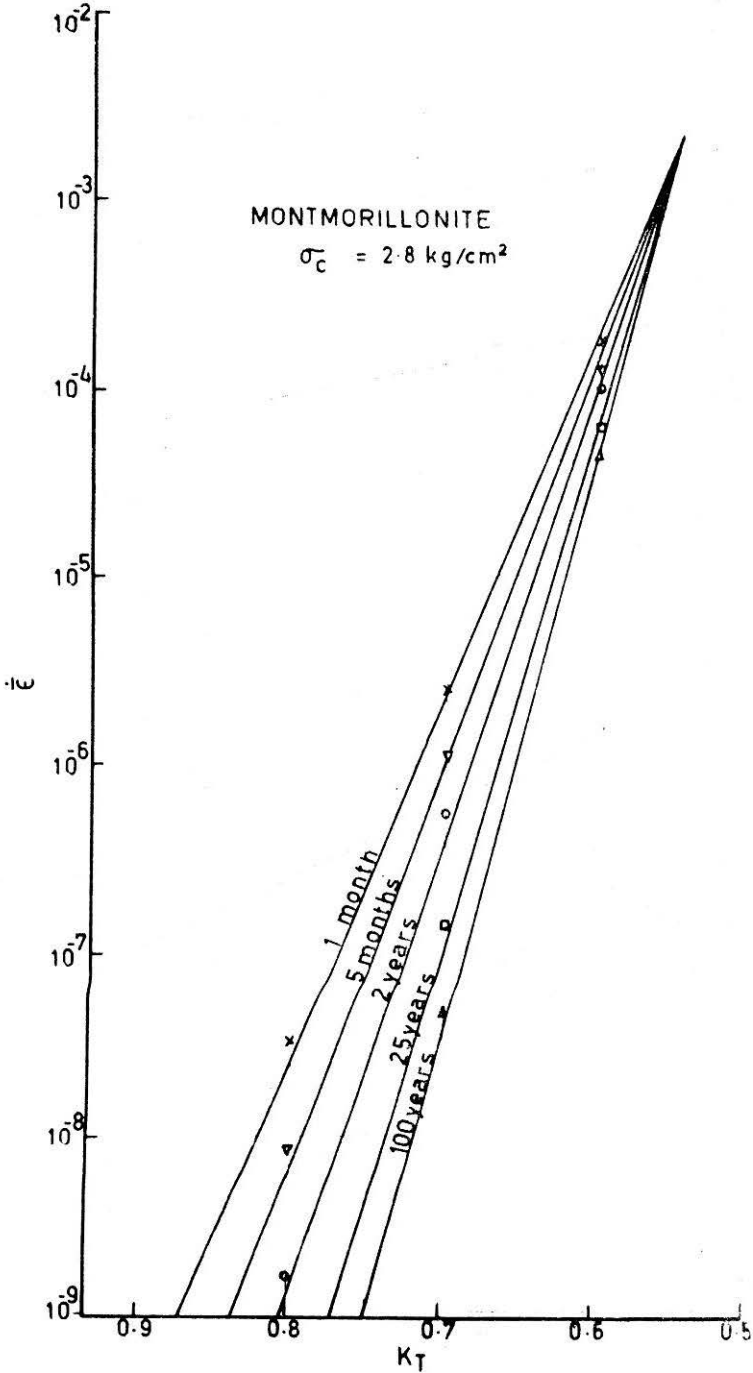
FIGURE 5(a) Strain Rate—Stress Ratio Plot

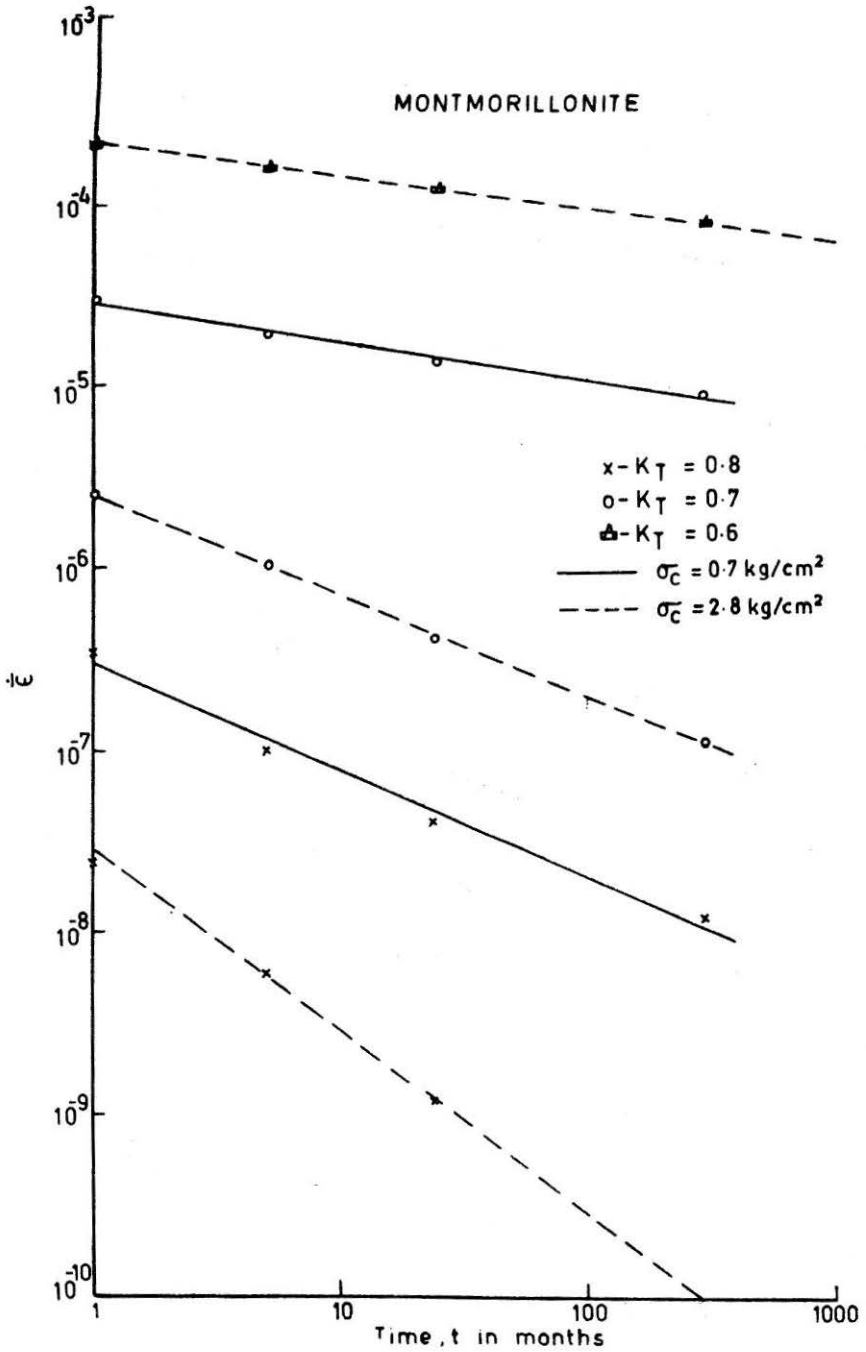**FIGURE 5(b) Strain Rate—Stress Ratio Plot**

FIGURE 5(c) Strain Rate—Time Plot

In order to relate the stress ratio K_T, strain rate $\dot{\epsilon}$ and time t, a new parameter "S" is introduced and is defined as

$$S = \frac{K_T - (K_T)\,\text{cr}}{\log \dot{\epsilon}_{cr} - \log \dot{\epsilon}} \qquad (4)$$

This parameter S and time t, when plotted on a log-log scale give rise to a straight line relationship (Fig 6). It is to be noted that the straight lines have different slopes and for the same time interval, with increasing consolidation pressure, S increases for kaolinite and decreases in the case of montmorillonite.

Fig. 14 shows the relation between consolidation pressure and the value of S at a particular time interval (10 days, S_{10}). They are found to be linear on the semi log scale.

Stress Strain-Time Relation

The equation for the straight lines connecting log S and log t (Figs. 6 can be written as

$$\frac{\log S - \log S_o}{\log t_o - \log t} = \alpha$$

where S_o is the value of S corresponding to a time $t = t_o$ and is the slope.

$$\frac{\log S/S_o}{\log t_o/t} = a$$
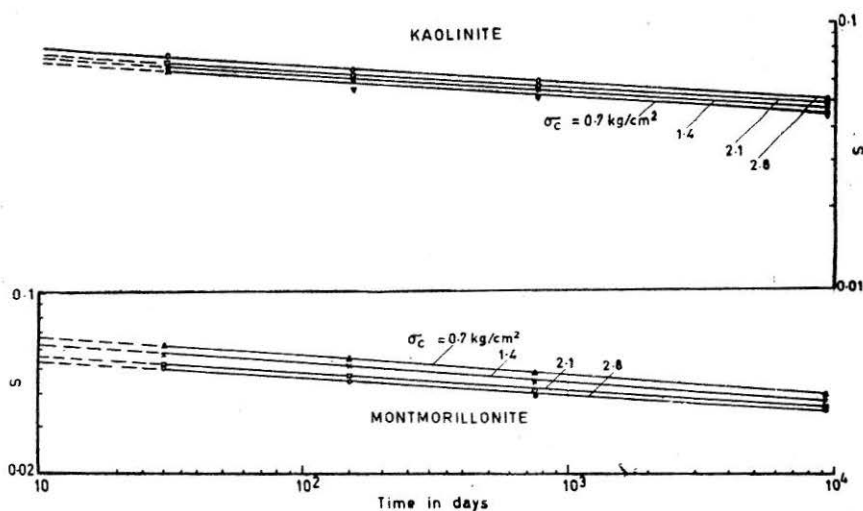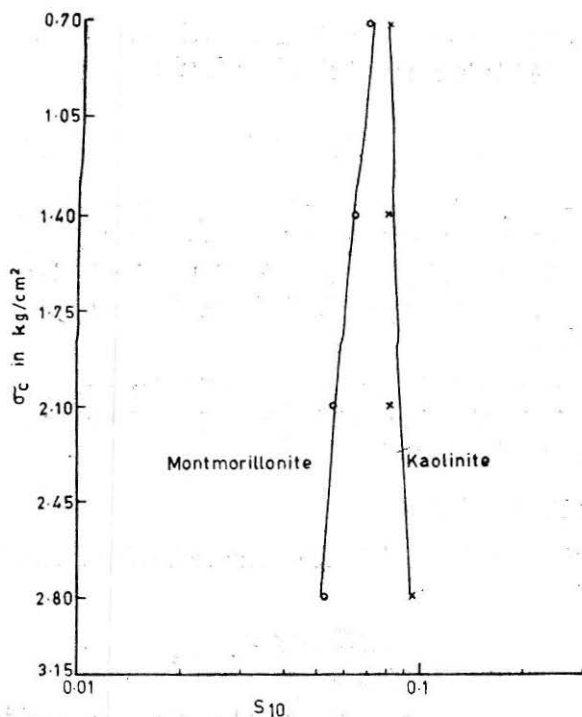
$$S = S_o \left(\frac{t_o}{t}\right)^\alpha \qquad (5)$$

FIGURE 6(a) S—Time Plot
FIGURE 6(b) S—Time Plot

FIGURE 7 Cell Pressure—S_{10} Plot

Since the relationship between cell pressure σ_3 and log S_{10} is linear, it follows that

$$\sigma_3 = \sigma_{3,1} + n \log S_{10} \tag{6}$$

where n is the slope of the "σ_3—$\log S_{10}$" plot, (Fig. 7) and $\sigma_{3,1}$ is the value of σ_3 at $S_{10}=1$.

From Eqn. (6)

$$\log_{10} S_{10} = \frac{\sigma_3 - \sigma_{3,1}}{n}$$

$$S_{10} = 10^{\frac{\sigma_3 - \sigma_{3,n}}{n}} \tag{7}$$

Replacing S_o and t_o by S_{10} and t_{10} in (5)

$$S = 10^{\frac{\sigma_3 - \sigma_{3,1}}{n}} \times \left(\frac{t_{10}}{t}\right)^{\alpha}$$

For a sample consolidated to a given cell pressure $\sigma_3 = \sigma_c$ (say) $\sigma_c - \sigma_{3,1}/n$ is a constant, and so, S_{10} is a constant.

Hence $S = S_{10} \left(\frac{t_{10}}{t}\right)^{\alpha}$

By definition $S = \dfrac{K_T - (K_T)\,cr}{\log \dfrac{\dot{\epsilon}_{cr}}{\dot{\epsilon}}}$ (from 4)

and so the above relation becomes

$$\frac{K_T - (K_T)\,cr}{\log \dfrac{\dot{\epsilon}cr}{\dot{\epsilon}}} = S_{10} \left(\frac{t_{10}}{t}\right)^{\alpha}$$

$$\frac{K_T - (K_T)_{cr}}{S_{10}} \left(\frac{t}{t_{10}}\right)^{\alpha} = \log \frac{\dot{\epsilon}_{cr}}{\dot{\epsilon}}$$

$$= 0.4343 \, \log_e \frac{\dot{\epsilon}_{cr}}{\dot{\epsilon}}$$

Rearranging the terms

$$\dot{\epsilon} = \dot{\epsilon}_{cr}\, e^{\displaystyle -2.3026 \frac{[K_T - (K_T)_{cr}]}{S_{10}} \left(\frac{t}{t_{10}}\right)^{\alpha}} \tag{8}$$

Interpretation of the Expression

The final equation for strain rate is a concise relationship which appears adequate enough for the description of the creep rate characteristics of clays over a wide range of plasticity, since it is found to hold good for kaolinite as well as montmorillonite. The parameter $\dot{\epsilon}_{cr}$ (*i.e.*, the critical strain rate) denotes the limit of creep rate for a soil under given conditions, since deformation rates in excess of this means strain softening (*i.e.*, increase of deformation rate with time) leading to rapid failure.

The expression for creep rate shows an exponential decrease of strain rate with time and this is in general agreement with that given by Awtar Singh and Mitchell (1968).

Discussion of Results

Strains

The key to this formulation is the experimentally observed fact that the logarithm of natural strain, when plotted against the logarithm of time results in linear relations excepting probably for those in the first minute or at the worst the second. Hence the published data of Campanalla (Awtar Singh and Mitchell, 1968) are presented as time (log scale) versus axial strain and, logarithm of natural strain vs logarithm of time to lend additional support to the linearisation (Fig 11.)

The plots 2 and 3 clearly bring out the influence of stress ratio. As can be expected, lower the value of stress ratio (K_T) higher is the resulting axial strain, since a low stress ratio means high intensity of deviatoric loading relative to the ambient pressure.

The variation of the slope, m (of line relating $\log_e \bar{\epsilon}$ with $\log e\ t$) is plotted against the total stress ratio, K_T in the inset of figures 2 and 3 for kaolinite and montmorillonite. Since there will be no creep under undrained condition when $K_T = 1$, it may be reasonable to assume zero value for m at $K_T=1$. This incidentally helps to extrapolate the curve backwards to the origin (dotted). One general feature of these inset curves concerns the nonlinear decrease of K_T with increase of m although the rate of decrease of K_T with increase of m is slight for montmorillonite with that for kaolinite being relatively more pronounced. Consideration of these two together will indicate a relatively lower value of $(K_T)_{cr}$ for kaolinite than for montmorillonite. The physical explanation is obvious in that the internal shear resistance for kaolinite being relatively more than that for montmorillonite, the critical level of deviatoric stress relative to ambient pressure is more for kaolinite than for montmorillonite. Using the same data, the variation of m, with σ_c, the consolidation pressure is reported in full lines for kaolinite in Fig. 8(a). Also plotted in the same figure are the dashed lines reporting the variation of m with σ_c for montmorillonite. It is seen that m decreases almost linearly with σ_c (over the range of σ_c studied) and the slope of these lines increases with the decrease of K_T value, both of which show that increased resistance to deformation increases with consolidation pressure more so at larger levels of deviatoric load (*i.e.*, less values of K_T). It may not be out of place to comment that the linear relation between $\log_e \bar{\epsilon}$ and $\log_e\ t$ for values of $m>1$ will be confined to those levels of strains up to which the deformation behaviour of the entire sample does not violate the compatibility condition much.

The same insets also present the variation of $\log_e C$ (intercept made on the $\log_e\bar{\epsilon}$ axis by the line relating $\log_e\bar{\epsilon}$ with $\log_e t$) with K_T the stress ratio. Since $\log_e C$ is nothing but $\log_e\bar{\epsilon}$ at $\log_e t=0$ (*i.e.*, the logarithm of natural strain at $t=1$), it is a measure of the strain recorded in one minute. Since, as already stated, there will be no creep under undrained condition with only ambient pressure (*i.e.* $K_T =1$), it is reasonable to assume zero value for $\bar{\epsilon}$ (as $\bar{\epsilon}=\log(1-\epsilon)$, $\epsilon= 0$ results in $\bar{\epsilon} = \log 1$, which is equal to zero) resulting in $\log_e\bar{\epsilon}$ taking a value of— ∞. This helps to extrapolate the curve forwards so that it meets $\log_e C$ at — ∞ when $K_T=1$. In other words, it becomes asymptotic with $\log_e C$ axis at $K_T =1$. Using the same data the variation of $\log_e C$ with σ_c is reported in full lines for kaolinite in Fig. 8(b). In the same figure, the variation of $\log_e C$ with σ_c for montmorillonite is also reported by dotted lines. It can be seen that $\log_e C$ decreases slightly
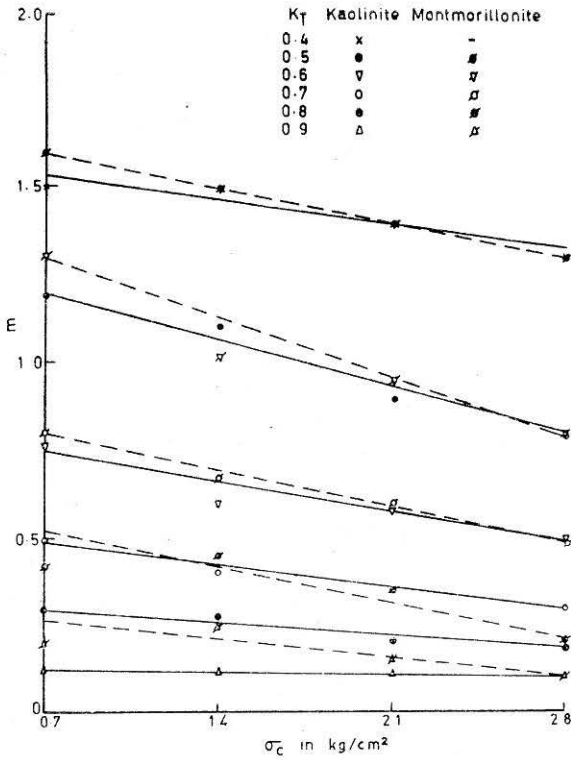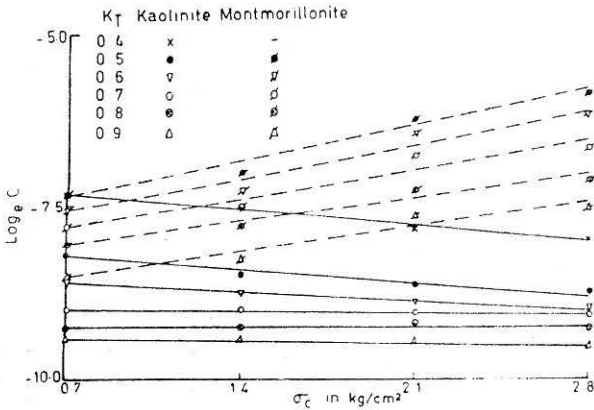
FIGURE 8(a) m—Cell Pressure Plot

FIGURE 8(b) C—Cell Pressure Plot

with consolidation pressure for kaolinite whereas it increases for mont-morillonite. A superficial look will indicate this as irreconcilable. How-ever, if it is remembered that $\log_e C$ (i.e., $\log_e \overline{\epsilon}$ at $t=1$) is a measure of the natural strain at $t=1$, it can be reasoned out that it will reflect the failure strain to some undefined scale. This could be deduced from the strain

levels of the *failed* samples. Comparison of the final values of $\log_e \bar{\epsilon}$ for $K_T=0.4$ in kaolinite (varying from—2.75 for $\sigma_c=0.7$ kg/cm² to—4.15 for $\sigma_c=2.8$ kg/cm²) and for $K_T=0.5$ in montmorillonite (varying from—2.65 at $\sigma_c=0.7$ kg/cm² to—2.24 at $\sigma_c=2.8$ kg/cm²) indicates the same trend of increase of failure strain in montmorillonite with σ_c and decrease in kaolinite. The opposing variation is thus logically related to the actual deformation behaviour.

Strain rates :

A study of results reported in Figs. 4(*a*), 4(*b*) 5(*a*) and 5(*b*) and the analysis of these results in Figs. 4(*c*) and 5(*c*) reveal that the strain rate decreases with increasing time, other things being equal for stress ratios less than the critical. This is probably due to the mobilization of the resist mechanisms with deformation. *i.e.* with time. It has been reported (Schmertmann, 1962) that mobilization of internal friction progresses with axial strain. This in turn offers increased resistance to deformation resulting in a decrease of strain rate with time. But, once the critical stress ratio (or the critical strain rate) is exceeded, the strain rate increases with time. This can be explained in terms of the well known strength versus axial strain plots wherein the strength increases with axial strain up to a peak value beyond which strength will decrease with further increase in axial strain. At large strains the sample tends to stabilize with a constant strength, known as the residual strength. Hence, an increase in strain (which results from increasing time) beyond that required for full mobilization of strength, results in a decrease in strength leading to increased deformation and deformation rates. As can be expected, strain rate increases with decreasing K_T for a given sample. At low consolidation pressures, the water content is more resulting in a major part of the deformation taking place as a result of the movements of the contacts through the double layer in addition to those of mineral to mineral contacts. But as the moisture content decreases as a result of increasing consolidation pressure, the deformation at mineral to mineral contact tends to predominate. This may explain the observed decrease in strain rate with increasing consolidation pressures.

For the same K_T time and consolidation pressure, strain rates are found to be higher in montmorillonite than in kaolinite. This is because, even at comparable levels of consolidation pressures, the moisture content of montmorillonite is very large compared to that of kaolinite.

The plots of $\dot{\bar{\epsilon}}$ vs K_T for different t values are replotted in Figs. 4(*c*) and 5(*c*). It is seen that the variation is a linear decrease in log-log scale which would also suggest a functional relationship of the type $\epsilon \, t^{-n} = a$ constant. This is not suggested as a new finding but as one indirectly varifying the correctness of the intermediatory steps suggested to evaluate the

parameters. As can be expected, for values of K_T around 0.8, the strain rate is low and its decrease with time is faster whereas for low values of K_T around 0.6 the strain rate is relatively high and hardly decreases with time. When K_T approaches $(K_T)_{cr}$, the strain rate will have to be essentially constant (since $m = 1$) and for values of K_T less than $(K_T)_{cr}$, strain rate will have to increase with time. The probable reasons for the decrease in strain rate with σ_c have already been discussed.

Critical Stress Ratio :

Fig. 9(a) reports the variation of the critical stress ratio $(K_T)_{cr}$ (as deduced from the insets of Figs. 2(a) through 3(b) for $m=1$) with consolidation pressure. The point of convergence of strain rate versus K_T for different periods (Figs. 4(a), 4(2), 5(a) and 5(b)) also defines $(K_T)_{cr}$ and the values so obtained are also reported in Fig. 9(a). The agreement in $(K_T)_{cr}$ found by both the methods seems to be quite satisfactory.
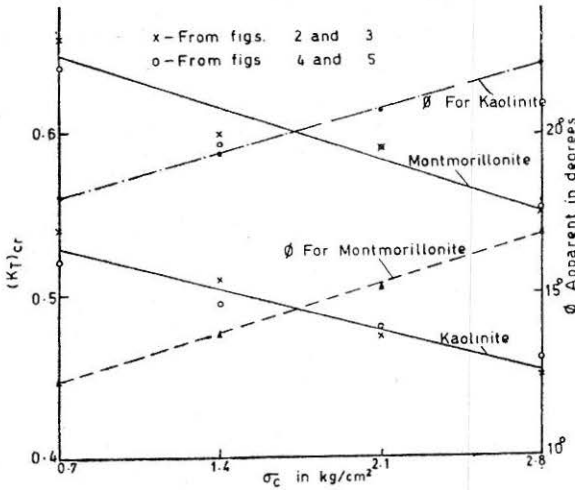

FIG. 9.1

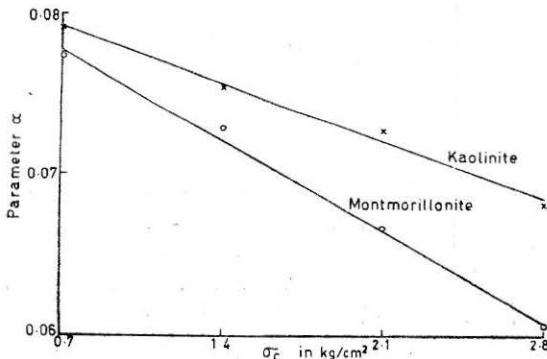**FIGURE 9(a) Stress Ratio/Apparent ϕ—Cell Pressure Plot**

FIGURE 9(b) α—Cell Pressure Plot

In a normally consolidated soil, the ratio of major to minor principal effective stresses at failure. $(\sigma_1'/\sigma_8')f$, is a direct measure of the angle of internal shear resistance since $(\sigma_1'/\sigma_3')=\tan^2 (45+\phi_f'/2)$ for Mohr-Coulomb criterion. As $(K_T)_{cr}$ refers to the inverse of such a ratio but in terms of total stresses, the apparent friction angle (i.e., ϕ, friction angle in terms of total stresses) is computed by an analogous relation $(\sigma_1/\sigma_{3cr} = \tan^2 (45+\phi/2)$. The variation of so computed ϕ (corresponding to the best lines drawn in Fig. 9(a) with σ_c is reported in dotted line for montmorillonite and in dashed and dotted line for kaolinite. The result, as can be expected, shows an increase of apparent friction angle with consolidation pressure.

Critical Strain Rates :

The critical strain rates obtained when $m=1$ and also got as the converging point from the plots of strain rate versus stress ratio are presented in Fig. 10 showing its variation with consolidation pressure. The values of $\dot{\epsilon}_{cr}$ predicted by both the methods agree between them reasonably well. It is found to decrease with consolidation pressure for kaolinite and increase with consolidation pressure for montmorillonite, and it is invariably higher in the case of montmorillonite than that of kaolinite. For this fundamentally differing behaviour in $\dot{\epsilon}_{cr}$ between kaolinite and montmorillonite, the explanation already advanced for the differences noticed in $\log_e C$ holds good. To have comparable strength levels, the moisture content of montmorillonite is very high compared to that of kaolinite. As a result, in montmorillonite the deformation occurs due to the movement of the contact points through double layers whereas the kaolinite it is mostly due to the movement of mineral to mineral contact points. This would explain the larger level of $\dot{\epsilon}_{cr}$ for montmorillonite. The opposing trends in $\dot{\epsilon}_{cr}$ with consolidation pressure exhibited by kaolinite ($\dot{\epsilon}_{cr}$ decreases with consolidation pressure) and montmorillonite ($\dot{\epsilon}_{cr}$ increases with consolidation pressure) can be essentially due to the basically differing trends of variation of failure strain with consolidation pressure in kaolinite and montmorillonite. In kaolinite, the failure strain is found to decrease with consolidation pressure whereas in montmorillonite it increases with consolidation pressure (G. MESRI, 1969).

Parameter α:

The variation of α (which appears in the final expression for creep rate) with consolidation pressure is presented in Fig. 9(b). It is found to decrease more or less linearly with consolidation pressure for both the soils studied. This can be seen to follow from the discussions made regarding the bahaviour of strain rate less than the critical, since, a decides the rate at which strain rate decreases with time. Since it is found that for montmorillonite the strain rate is always higher than that for kaolinite under
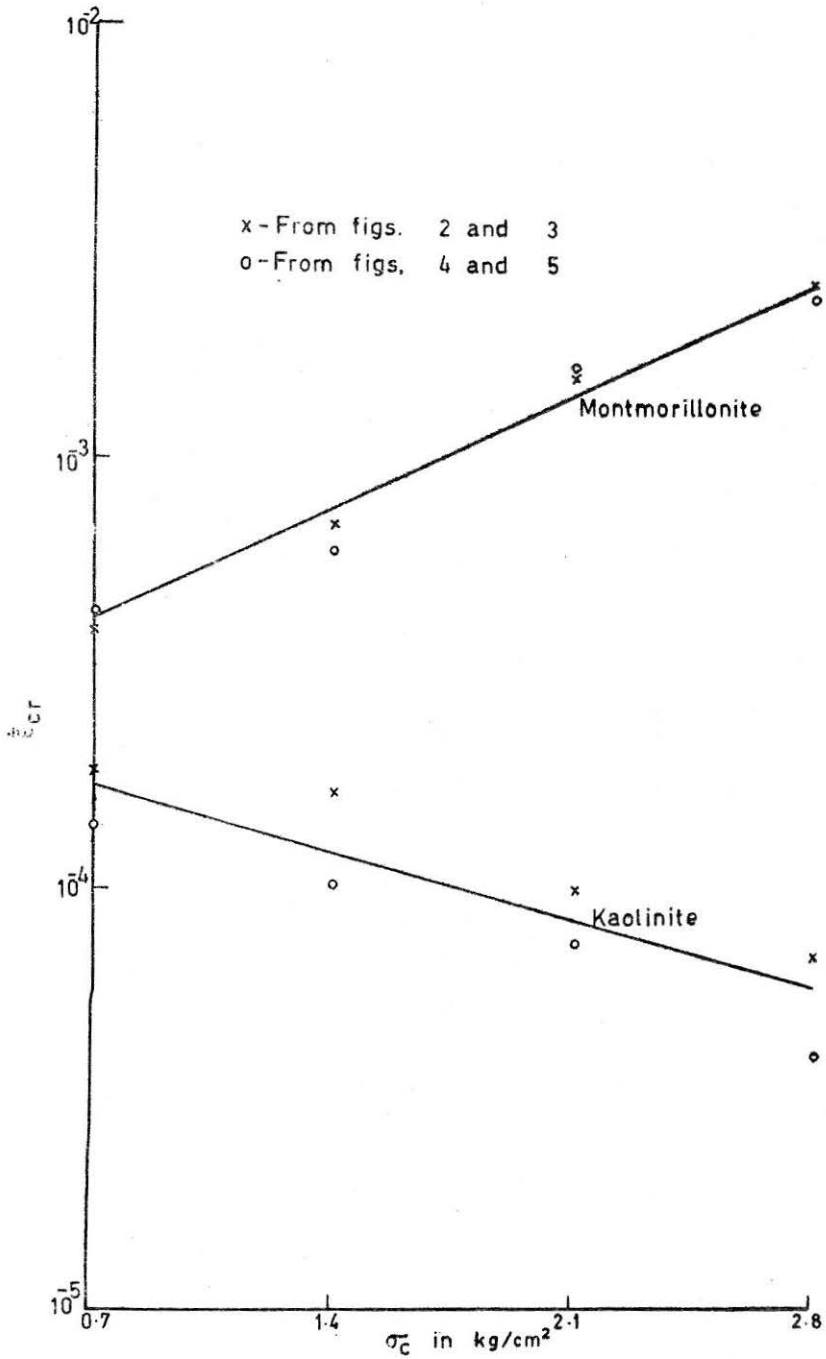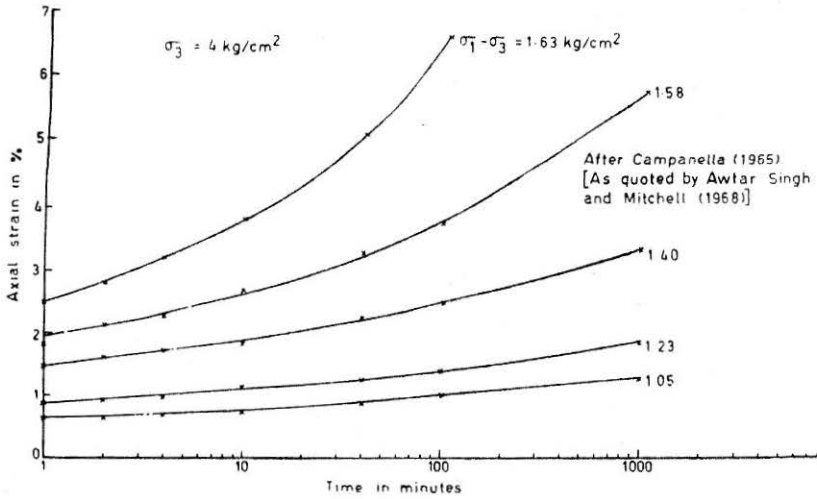
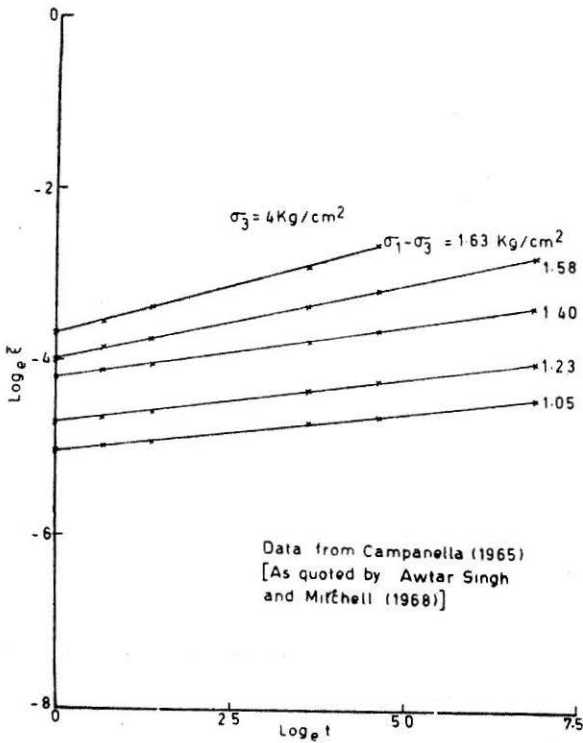FIGURE 10 Critical Strain Rate—Cell Pressure Plot

FIGURE 11(a) Strain—Time Plot

FIGURE 11(b) Strain—Time Plot.

same conditions of stress ratio and consolidation pressure, it is logical to expect a to be less as well as to decrease faster in montmorillonite than in kaolinite as confirmed by the results reported in Fig. 9(b).

Conclusions

The problem of creep in soils has been mostly tackled by mathematical models based on limited experimental data. Literature abounds to show that even in such approaches certain nonlinear portions are sacrificed the mathematical formulation. Hence a model is herein chosen to cover the entire range of the time-strain response based on the experimental observation that the natural strain linearises with time on log-log scale. The linearisation is shown to hold good for the entire range of response for extreme cases of clay behaviour by conducting studies on kaolinite and montmorillonite. Another advantage of this approach is the facility with which the involved parameters could be determined. For the soils tested, the parameters in the expression developed for undrained creep strain rate in a sample consolidated to a given ambient pressure and subject to a given total stress ratio are evaluated and their variation with stress level, soil type etc. has been explained in terms of probable changes at particle level. Two important parameters, viz., critical stress ratio and the associated strain rate, deduced by two independent techniques have shown reasonable agreement between themselves and this is taken to lend indirect support to the soundness of the approach. It may be mentioned that highly impervious clays under sustained loading undergo undrained creep deformation.

Acknowledgements

References

AWTAR SINGH and MITCHELL, J.K. (1968) : "General Stress Strain Time Function for Soil", *Proc ASCE*, Vol. 94, SM. 1, 21-46.

KAVAZANJIAN, E. and MITCHELL, J.K. (1980): "Time Dependent Deformation Behaviour of Clays", *Proc. ASCE*, Vol. 106, GT. 6: 611-630.

MESRI, G. (1969): "Engineering Properties of Montmorillonite". Ph. D. Thesis, University of Illinois, Urbana.

SCHMERTMANN, J.H. (1962): "Comparisons of one and two Specimen CFS Tests," *Proc ACSE*, Vol. 88, SM 6: 169-205.

SEKIGUCHI, H. (1984): "Theory of Undrained Creep Rupture of Normally Consolidated Clay based on Elasto-Viscoplasticity", *Soils and Foundations*, Vol. 24, No. 1: 129-147.